Supplementary Information

Deep oxidative desulfurization of model fuel catalyzed by polyoxometalates anchored on amine-functionalized ceria doped MCM-41 under molecular oxygen

Chaowei Wang[a], Zhe Liu[a], Ruimin Gao[b], Jinhua Liu[a], Siying An[a], Ronglan Zhang[a], Jianshe Zhao[a*]

[a] Key Laboratory of Synthetic and Natural Functional Molecule Chemistry of Ministry of Education, Shaanxi Key Laboratory of Physico-Inorganic Chemistry, College of Chemistry & Materials Science, Northwest University, Xi' an 710069, China

[b] Research Institute of Shaanxi Yanchang Petroleum Group Corp. Ltd., Xi'an 710075, China

*Corresponding author.

E-mail: jszhao@nwu.edu.cn

Table S1. ICP results of different catalysts.

Catalyst	W[a] (wt%)	V[a] (wt%)	W/V (mol ratio)	POM[b] (wt%)
10 wt% PW_9V_3/APTES-CeM-50	5.35	0.49	3.03	8.91
20 wt% PW_9V_3/APTES-CeM-50	11.47	1.06	3.00	19.12
30 wt% PW_9V_3/APTES-CeM-50	17.12	1.58	2.99	28.53
40 wt% PW_9V_3/APTES-CeM-50	23.25	2.15	3.00	38.75
50 wt% PW_9V_3/APTES-CeM-50	27.94	2.58	2.99	46.57
30 wt% PW_9V_3/CeM-50	10.11	0.94	3.00	16.83
After used 8 times	12.98	1.20	3.00	21.63

[a] As tested by ICP-AES analysis.

[b] As calculated from the ICP-AES results.

Table S2. APTES amounts of different catalysts.

Sample	Amine[a] (mmol/g)
CeM-50	0
APTES-CeM-50	4.2
30 wt% PW_9V_3/APTES-CeM-50	4.2

[a] As obtained according to TG method. The unit of amine amount is mmol amine/g CeM.

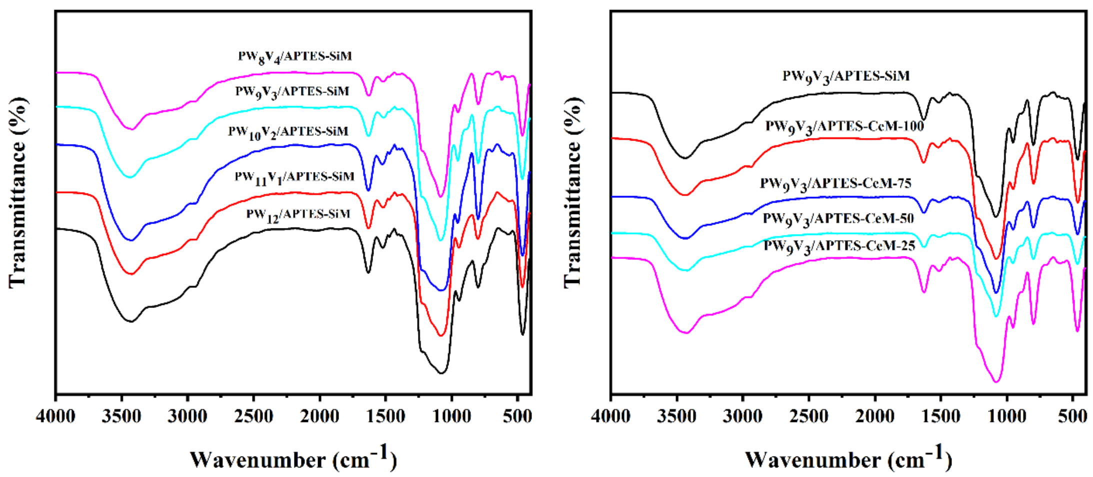

Fig. S1. FT-IR spectra of POM/APTES-SiM and PW_9V_3/APTES-CeM.

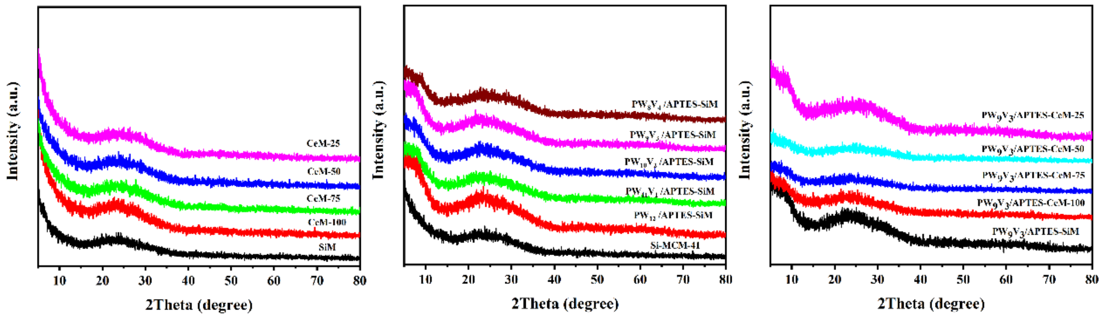

Fig. S2. XRD spectra of POM/APTES-SiM and PW_9V_3/APTES-CeM.

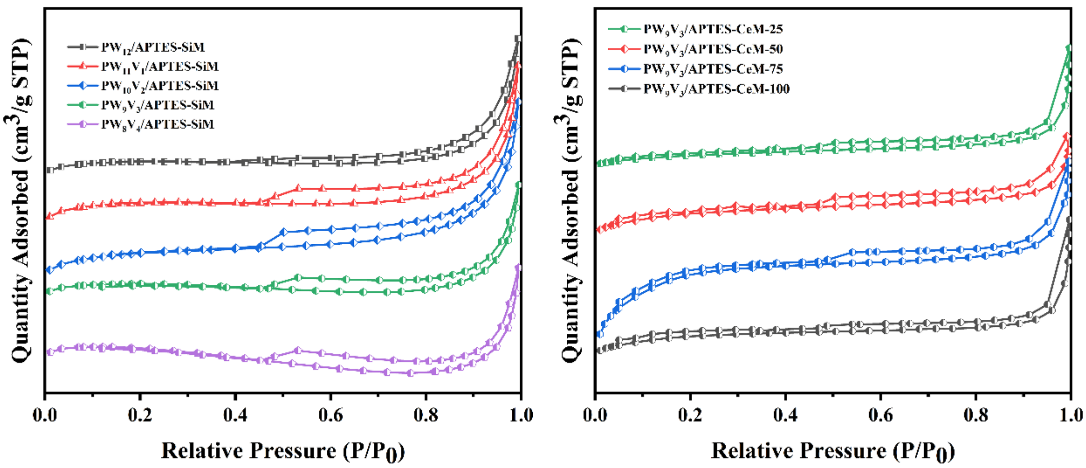

Fig. S3. Nitrogen adsorption-desorption isotherms of POM/APTES-SiM and PW_9V_3/APTES-CeM.

Table S3. Textural properties of POM/APTES-SiM and PW_9V_3/APTES-CeM.

Sample	S_{BET} (m^2/g)	V_P (cm^3/g)	D_P (nm)
PW_{12}/APTES-SiM	297	0.415	2.88
$PW_{11}V_1$/APTES-SiM	292	0.399	2.89
$PW_{10}V_2$/APTES-SiM	286	0.381	2.84
PW_9V_3/APTES-SiM	274	0.362	2.81
PW_8V_4/APTES-SiM	283	0.374	2.85
PW_9V_3/APTES-CeM-100	258	0.358	2.80
PW_9V_3/APTES-CeM-75	245	0.341	2.76
PW_9V_3/APTES-CeM-50	233	0.328	2.74
PW_9V_3/APTES-CeM-25	186	0.293	2.67

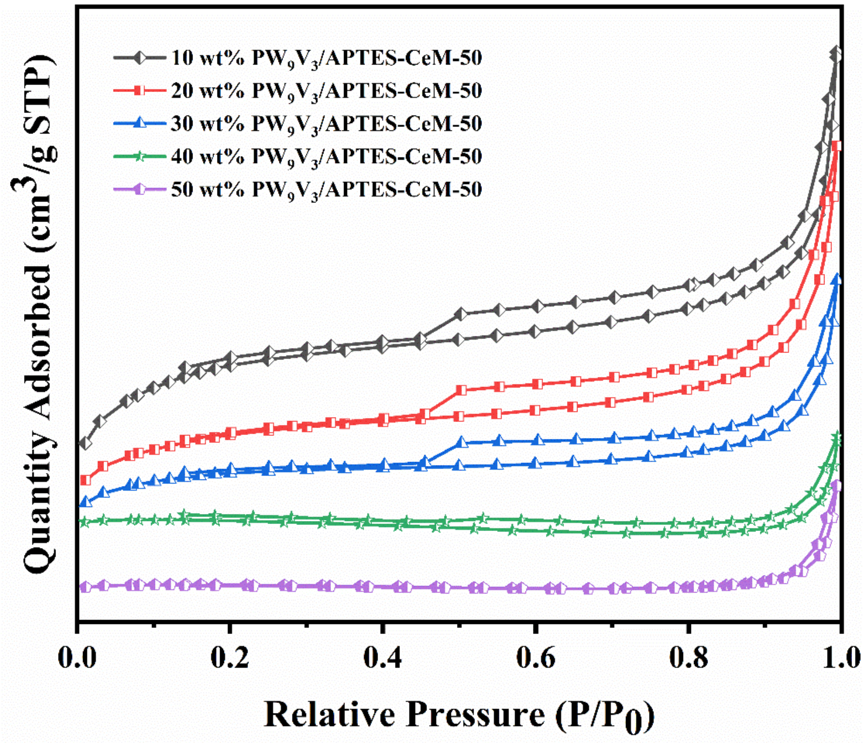

Fig. S4. Nitrogen adsorption-desorption isotherms of the 10-50 wt% PW_9V_3/APTES-CeM-50 catalysts.

Table S4. Textural properties of the 10-50 wt% PW_9V_3/APTES-CeM-50 catalysts.

Sample	S_{BET} (m^2/g)	V_P (cm^3/g)	D_P (nm)
10 wt% PW_9V_3/APTES-CeM-50	536	0.476	2.90
20 wt% PW_9V_3/APTES-CeM-50	374	0.391	2.83
30 wt% PW_9V_3/APTES-CeM-50	233	0.328	2.74
40 wt% PW_9V_3/APTES-CeM-50	108	0.249	2.68
50 wt% PW_9V_3/APTES-CeM-50	67	0.195	2.63

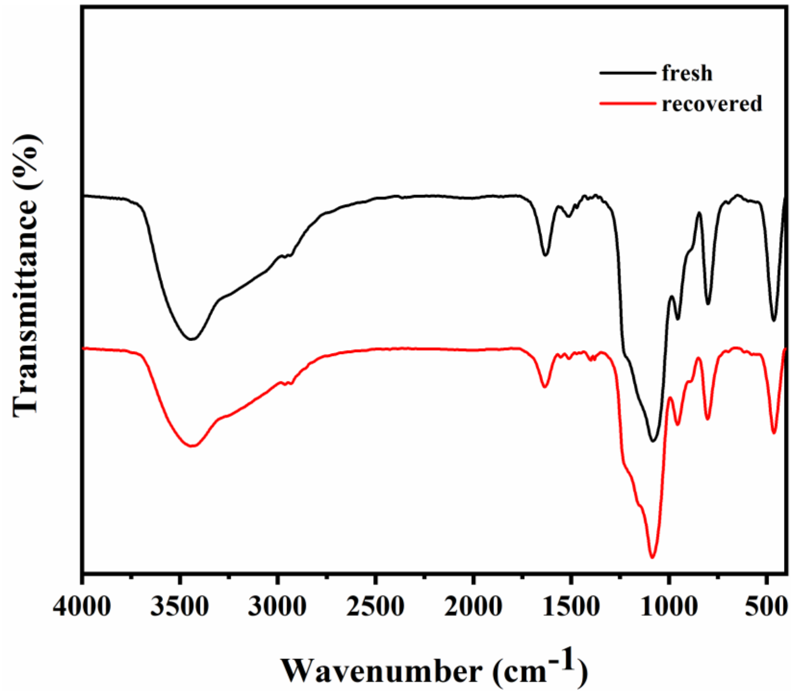

Fig. S5. FT-IR spectra of the fresh and after used 8 times catalyst.

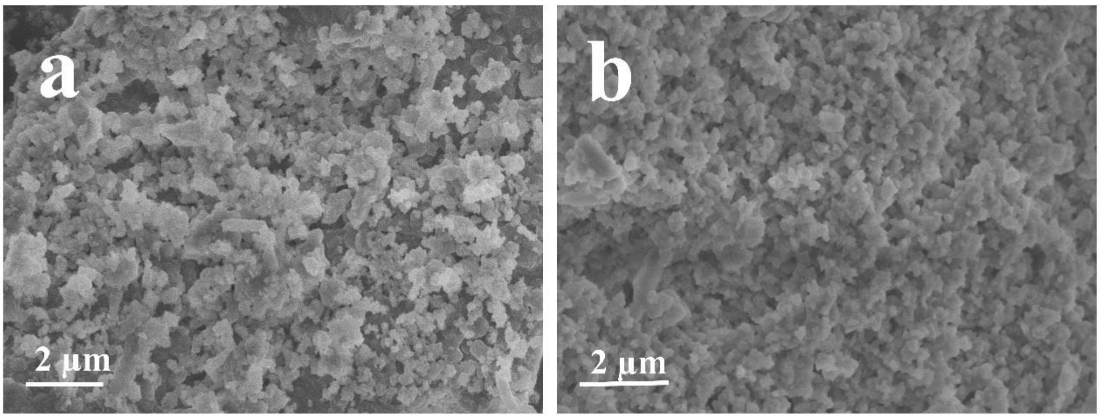

Fig. S6. SEM images of the (a) fresh and (b) after used 8 times catalyst.

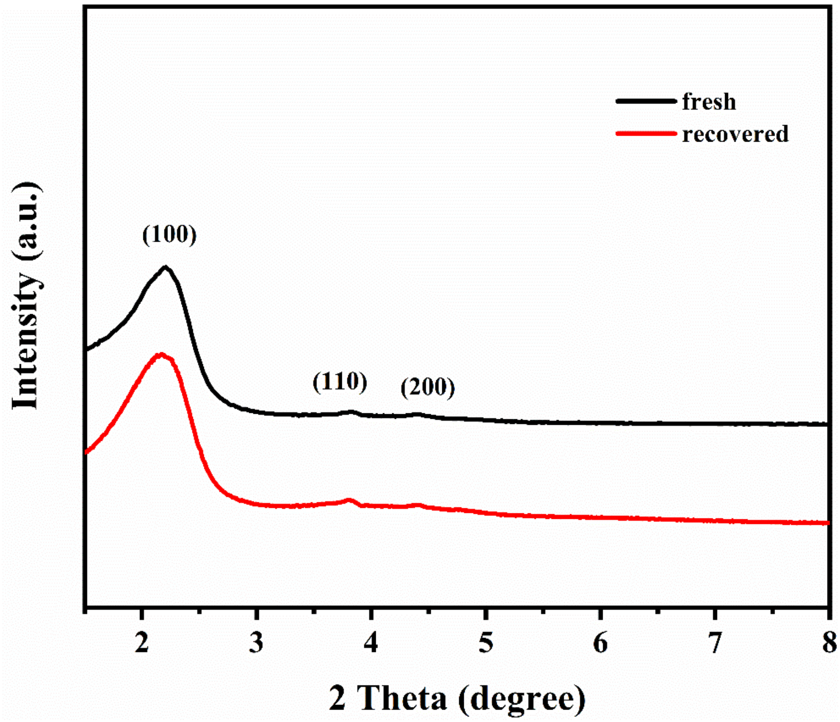

Fig. S7. Low angel XRD patterns of the fresh and after used 8 times catalyst.

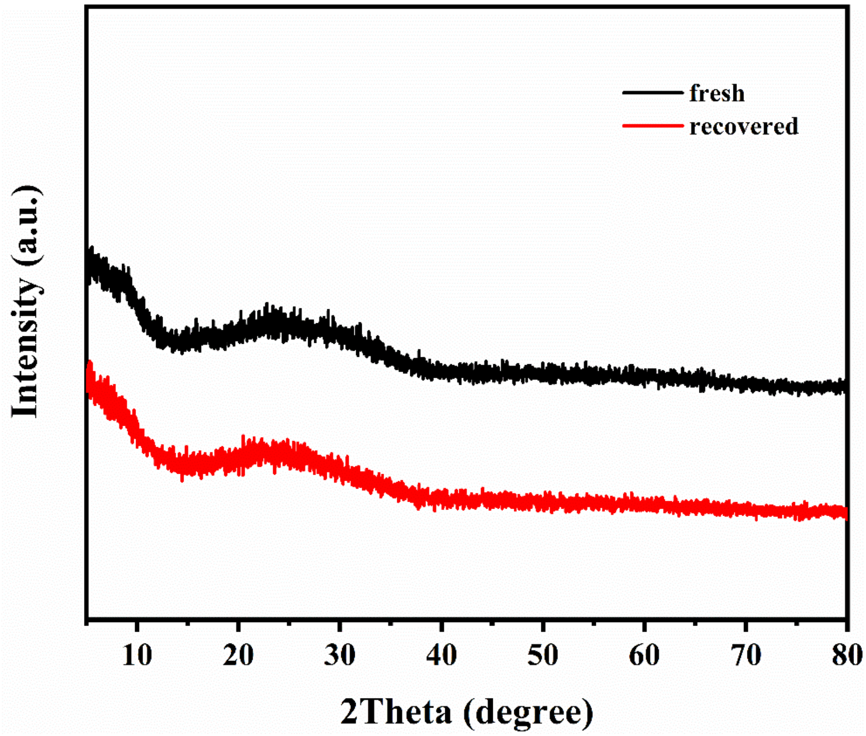

Fig. S8. Wide angel XRD patterns of the fresh and after used 8 times catalyst.

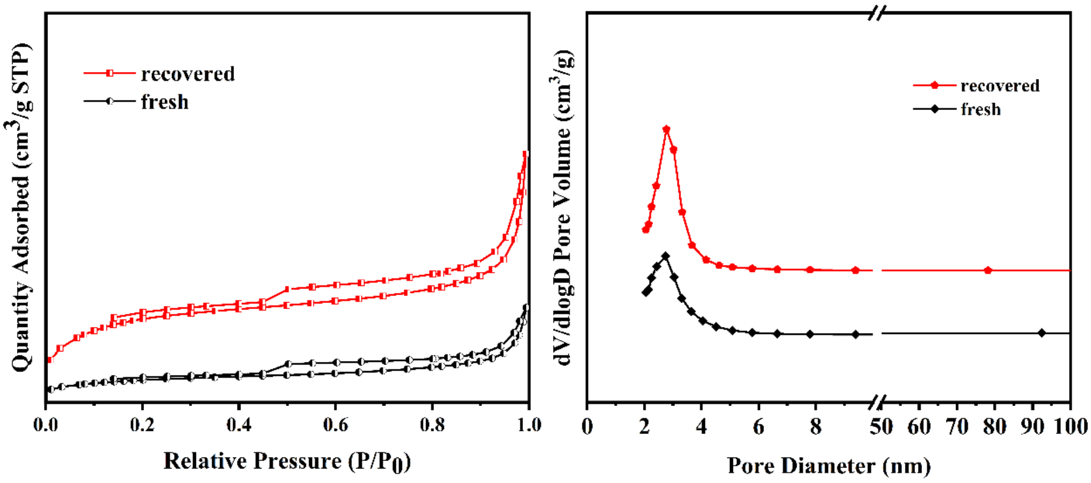

Fig. S9. Nitrogen adsorption-desorption isotherms and BJH pore size distribution curves of the fresh and after used 8 times catalyst.

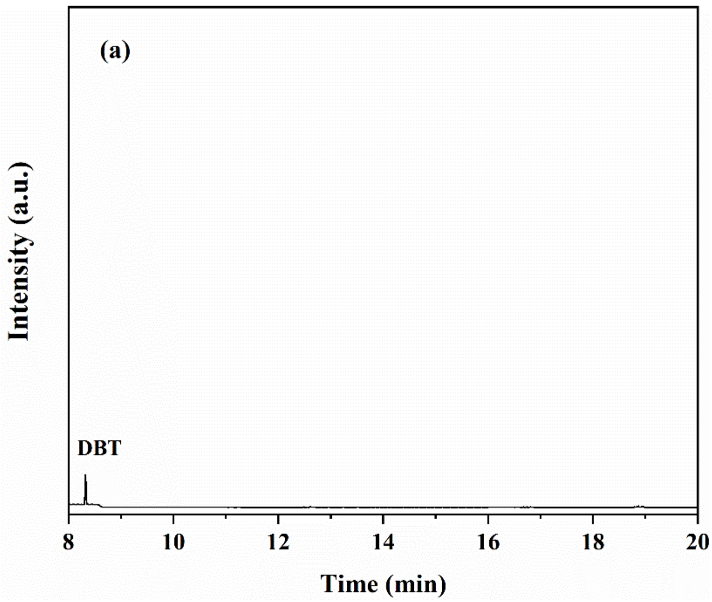

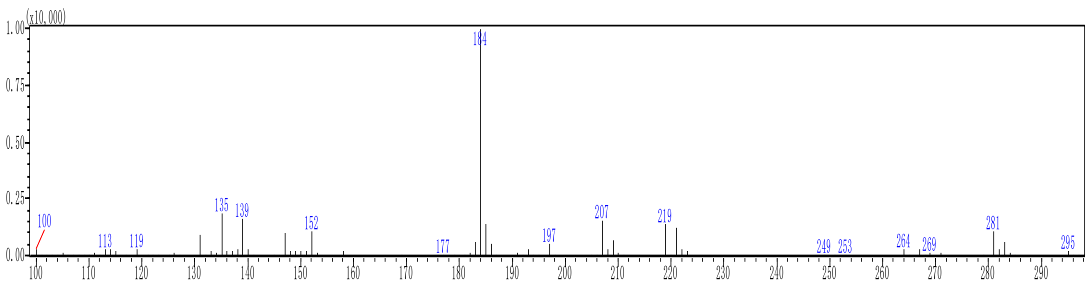

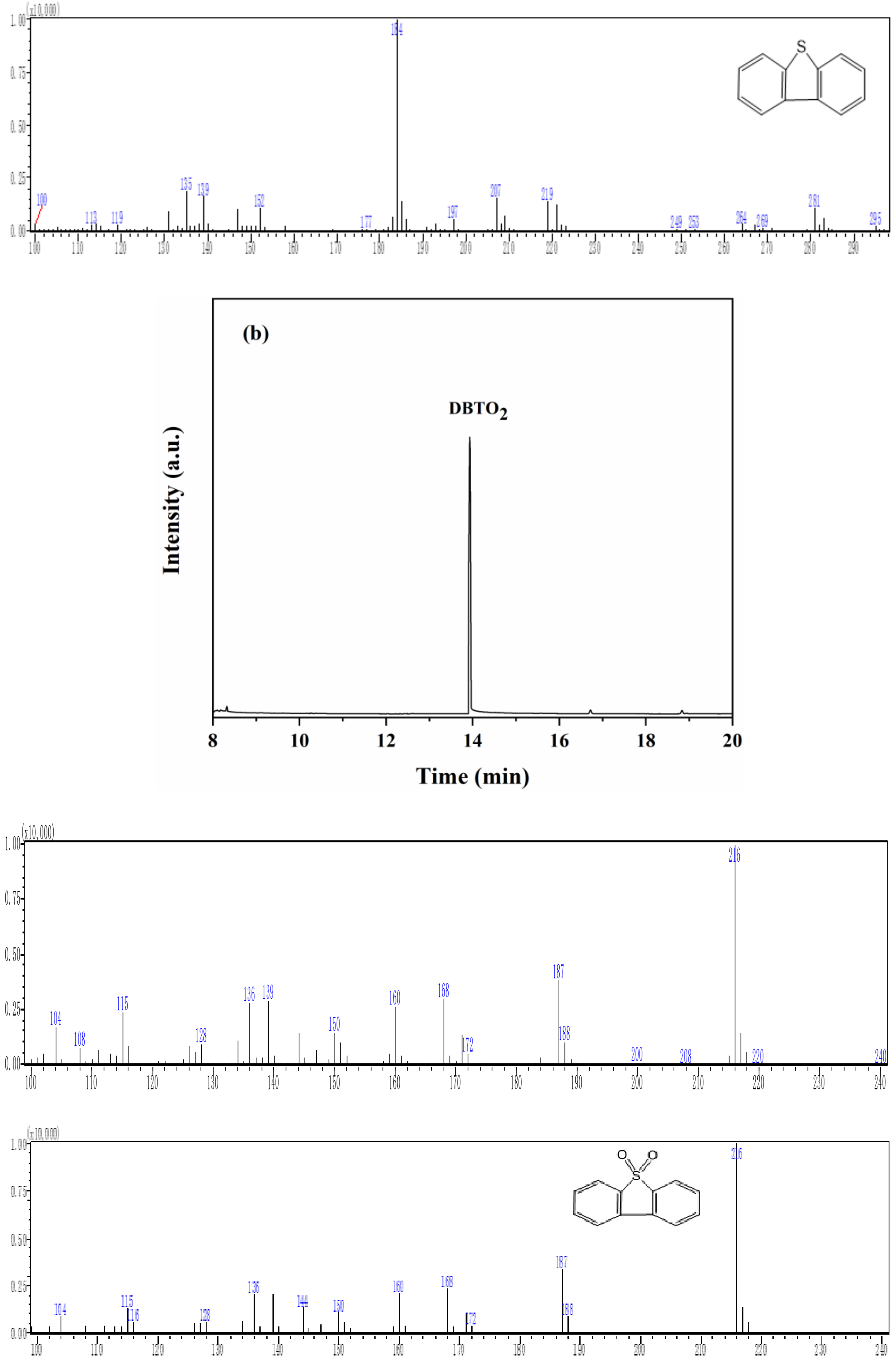

Fig. S10. The GC-MS analysis of the product after ODS. (a) oil phase, (b) CH_3CN phase.

Table S5. The kinetic data of different reaction temperature.

Temperature/°C	Rate constant k/min^{-1}	Correlation factor R^2
50	0.00905	0.99132
60	0.01208	0.98763
70	0.01596	0.99221
80	0.02481	0.99732

Table S6. The comparison between ODS results of different POM based catalysts.

Catalyst	Oxidant	Temperature/ °C	DBT conversion/%	Reference
Ag-POM/SWNTs	H_2O_2	20	98.9	S1
$K_6P_2W_{18}O_{62}$/GO	Air	60	96.10	S2
HPMo/C	H_2O_2	60	100	S3
HPW@MOFs	O_2	90	90	S4
HPW/MgAl-LDH-DBS [a]	H_2O_2	60	99.81	S5
$H_8PV_5Mo_7O_{40}$	O_2	120	99	S6
$(TBA)_4PW_{11}Fe$@PbO [b]	CH_3COOH/H_2O_2	60	97	S7
CNTs@MOF-$Mo_{16}V_2$	O_2	80	98.30	S8
PW_9V_3/APTES-CeM-50	O_2	80	99.26	This work

[a] This catalyst represents the phosphotungstic acid (HPW) supported the sodium dodecyl benzene sulfonate (SDBS) modified layered double hydroxides (LDH).

[b] This catalyst means a tetra(n-butyl)ammonium salt of iron-substituted phosphotungstate@lead oxide composite.

Reference

S1 H. Zhang, X. Xu, H. Lin, Din, A. U. M, H. Wang and X. Wang, *Nanoscale*, 2017, **9**, 13334-13340.

S2 S. Dou and R. Wang, *New J. Chem.*, 2019, **43**, 3226-3235

S3 R. Ghubayra, C. Nuttall, S. Hodgkiss, M. Craven, E. F. Kozhevnikova and I. V. Kozhevnikov, *Appl. Catal., B*, 2019, **253**, 309-316.

S4 J. W. Ding and R. Wang, *Chin. Chem. Lett.*, 2016, **27**(5), 655-658.

S5 P. Huang, A. Liu, L. Kang, M. Zhu and B. Dai, *New J. Chem.*, 2018, **42**, 12830-12837.

S6 B. Bertleff, J. Claußnitzer, W. Korth, P. Wasserscheid, A. Jess and J. Albert, *ACS Sustainable Chem. Eng.*, 2017, **5**(5), 4110-4118.

S7 M. A. Rezvani, S. Khandan and N. Sabahi, *Energy Fuels*, 2017, **31**, 5472-5481.

S8 Y. Gao, Z. Lv, R. Gao, G. Zhang, Y. Zheng and J. Zhao, *J. Hazard. Mater.*, 2018, **359**, 258–265.